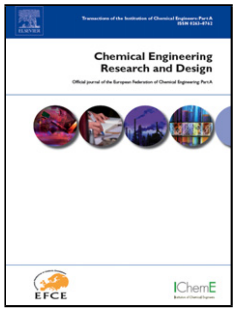

Title: Influence of surface tension gradient on liquid circulation time in a draft tube airlift reactor

Author: Boris Albijanic Snehamoy Chatterjee Nimal Subasinghe Mohammad Waqar Ali Asad

PII: S0263-8762(16)30195-2
DOI: http://dx.doi.org/doi:10.1016/j.cherd.2016.07.016
Reference: CHERD 2340

To appear in:

Received date: 3-2-2016
Revised date: 13-6-2016
Accepted date: 18-7-2016

Please cite this article as: Albijanic, B., Chatterjee, S., Subasinghe, N., Asad, M.W.A.,Influence of surface tension gradient on liquid circulation time in a draft tube airlift reactor, *Chemical Engineering Research and Design* (2016), http://dx.doi.org/10.1016/j.cherd.2016.07.016

Graphical Abstract

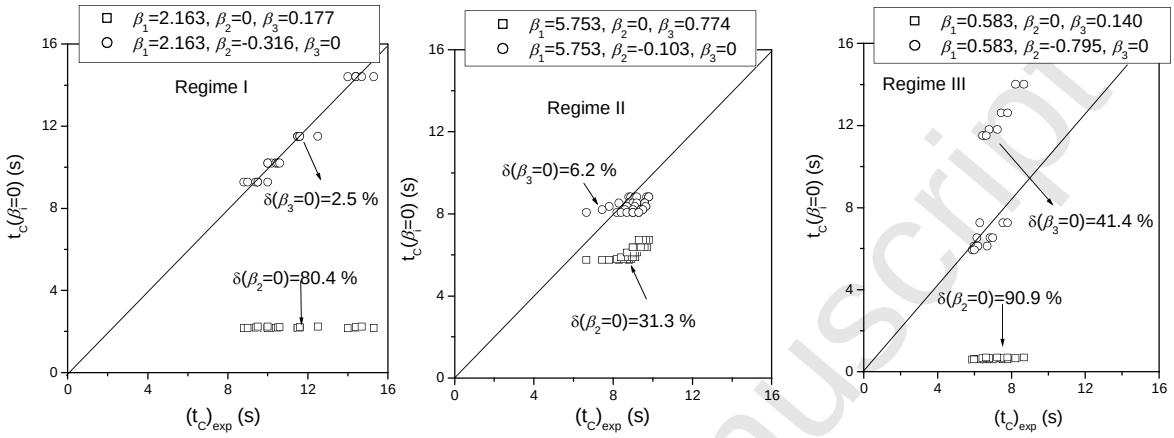

Highlights

- Circulation time of dilute alcohol solutions in an airlift reactor was determined.
- Three different bubble regimes in the downcomer were observed.
- A paired sample t-test confirmed the presence of three hydrodynamic regimes.
- The superficial gas velocity is the dominant factor for all hydrodynamic regimes.
- The effect of surface tension gradient is particularly significant in Regime II.

Influence of surface tension gradient on liquid circulation time in a draft tube airlift reactor

Boris Albijanic[1*], Snehamoy Chatterjee[2*], Nimal Subasinghe[1], Mohammad Waqar Ali Asad[1]

[1]Department of Mining Engineering and Metallurgical Engineering, Curtin University, Kalgoorlie, WA 6430, Australia

[2]Department of Geological and Mining Engineering and Sciences, Michigan Technological University, Houghton, MI 49931, USA

boris.albijanic@curtin.edu.au

schatte1@mtu.edu

Abstract

This paper investigates the impact of surface tension gradient on liquid circulation time in a draft tube airlift reactor using dilute alcohol solutions. The experimental work proves the existence of three bubble regimes (*Regime I*: no bubbles in the downcomer; *Regime II*: a stagnant swarm of bubbles in the downcomer; *Regime III*: circulation of bubbles through the reactor) in the downcomer. A paired sample *t-test* also confirms the presence of these hydrodynamic regimes. The liquid circulation time results can be predicted from a proposed correlation which has two independent variables: surface tension gradient in dilute alcohol solutions as a variable representing the physical property of liquid phase, and superficial gas velocity as a hydrodynamic variable. The statistical evaluation quantifies the influence of each independent variable through its elimination from the proposed correlation. Additionally, the second approach compares the rate of change in the liquid circulation time with respect to the surface tension gradient and the superficial gas velocity. It was found that the superficial gas velocity was more significant variable than the surface tension gradient for all three hydrodynamic regimes. The influence of the surface tension gradient on the liquid circulation time was insignificant at lower superficial gas velocity due to a negligible amount of bubbles in the reactor. However, the opposite was true at higher superficial gas velocity. It is evident that in the draft tube airlift reactor environment, the effect of surface tension gradient on liquid circulation time largely depends on superficial gas velocity.

Key words: Airlift reactors, dilute alcohol solutions, circulation time, hydrodynamic regimes, statistical modelling

1. Introduction

Airlift reactors are widely used in fermentation industry and wastewater treatment. In these reactors, the properties of liquid phase may have a profound effect on the bubble size,

consequently influencing the hydrodynamic and mass transfer behaviour of the reactor (Albijanic et al., 2007). If surface tension of dilute aqueous solutions of alcohols is the only physical property of liquid phase that exhibits significant difference from water, these solutions can be used to simulate the behaviour of these reactors.

The addition of a small amount of alcohols in aqueous solutions strongly suppresses coalescence between bubbles due to the formation of a rigid monolayer around bubbles, making their surfaces immobile (Al-Masry and Dukkan, 1997; Krishna et al., 2000). When a bubble rises through a liquid, adsorbed alcohol molecules move to the back of the bubble, and cause the surface tension gradient that resists the tangential shear stress. Therefore, the increase in the drag force on the bubble reduces the bubble rise velocity (Krishna et al., 2000), which improves the entrainment of bubbles in the downcomer section of the reactor (Albijanic et al., 2007). The presence of bubbles in the downcomer may have a significant effect on liquid circulation because the driving force for liquid circulation is directly proportional to the difference between the gas holdup in the riser and that in the downcomer (Albijanic et al., 2007, Sijacki et al., 2010).

Liquid circulation not only facilitates mixing of solids, but also it improves heat and mass transfer in airlift reactors, and consequently, the determination of liquid circulation in these reactors becomes very important. In previous studies, the circulation time of dilute alcohol solutions in draft tube airlift reactors has been determined experimentally (Fields and Slater, 1983; Weiland, 1984; Petrovic et al., 1991; Kennard and Janekeh, 1991; Freitas and Teixeira, 1998; Albijanic et al., 2007). However, the impact of physical properties of dilute alcohol solutions on liquid circulation time has not been statistically quantified. Realizing the potential value of this work, in the following sections, we present a review of the relevant previous studies, the methodology that describes both experimental and statistical approaches, a detailed discussion on results implementing both approaches, and conclusions.

2. Previous work

Table 1 presents a concise review of studies on the liquid circulation time for the dilute alcohol solutions in the draft tube airlift reactors. The literature reveals that the factors like geometry and the type of spargers establish whether the addition of alcohols affects the liquid circulation time.

Table 1. A review of investigations of the liquid circulation time for the dilute alcohol solutions in the draft tube airlift reactors.

Author	D (cm)	D_R/D (%)	Type of sparger	Liquid
1. Fields and Slater, 1983	15.2	63	Porous plate	1% ethanol
2. Weiland, 1984	20	59, 74, 88	Sinter plate, d=150-200 μm	Water 0.22% 2-propanol
3. Petrovic et al., 1991	20	40, 50, 75	Perforated plate, 19 holes, d=1 mm	Water 0.5% n-butanol
4. Kennard and Janekeh, 1991	22	45	Sinter plate, d=150 μm	Water 10 g/L ethanol+ 0.5 g/L CMC
5. Freitas and Teixeira, 1998	14.2	119	Perforated plate, 30 holes, d=1 mm	Water 10 g/L ethanol
6. Albijanic et al., 2007	10.6	51	Single orifice, d=4 mm	water, 1% methanol, ethanol, n-propanol, isopropanol, n-butanol
7. This work	10.6	51	Single orifice, d=4 mm	water, 0.5% methanol, ethanol, n-propanol, isopropanol, n-butanol

D_R – diameter of draft tube
D – diameter of column

In this context, Chakravarty et al. (1974) reported that the influence of added alcohol on the liquid circulation time was negligible even though the surface tension of liquid phase changed from 0.049 to $0.072\ N/m$. The reason is that these authors used a short draft tube ($0.04\ m$), causing considerable reduction in the driving force for liquid recirculation. Freitas and Teixeira (1998) also reported similar observations since their reactor had a large separator section which reduced the entrainment of bubbles in the downcomer. On the contrary, Petrovic et al. (1991) and Albijanic et al. (2007) used a long draft tube and observed that the addition of small amount of alcohols increases the liquid circulation time considerably, mainly due to extensive entrainment of bubbles in the downcomer which reduced the driving force for the liquid circulation.

Apart from the geometry of the airlift reactors, the type of the spargers may affect the hydrodynamic behaviour of liquid phase. For example, Weiland (1984) found that the circulation time of dilute alcohol solutions was 50% higher as compared to that in tap water at lower

superficial gas velocities. The reason is that the sinter plate resulted in improved entrainment of bubbles in the downcomer. However, at higher superficial gas velocities, the circulation time of dilute alcohol solutions remained 25% lower than that in tap water due to the intense turbulence of the liquid phase.

In the context of the prediction of circulation time of dilute alcohol solutions, Albijanic (2006) used the correlation that accounts for the superficial gas velocity, the surface tension of alcohol solutions, and the number of carbon atoms in the molecule of alcohol. Although this correlation successfully described the experimental data, the surface tension of alcohol solutions and the number of carbon atoms in the molecule of alcohol are not independent variables. Namely, surface tension of dilute solutions of alcohol with a higher number of carbon atoms is lower than that of alcohol with a lower number of carbon atoms. It is important to highlight that surface tension better represents the physical properties of dilute alcohol solutions than the number of carbon atoms in the molecule of alcohols because different isomers of the same molecule of alcohol have the same number of carbon atoms, but dilute solutions of these isomers may have different values of surface tension (e.g. surface tension for 1% propanol is $61.8 \times 10^{-3}\ N/m$, while that for 1% isopropanol is $59.6 \times 10^{-3}\ N/m$ (Albijanic et al., 2007)). For that reason, Albijanic et al. (2007) proposed the correlation with two independent variables: superficial gas velocity and surface tension gradient, and their proposed correlation successfully predicted the experimental data.

3. Methodology

3.1. Experimental setup and physical properties of liquid phase

The experiments were performed in an airlift reactor that consists of an inner glass tube $(D_R = 0.053\ m;\ H = 1.3\ m)$ and an outer glass tube $(D = 0.106\ m;\ H = 2.5\ m)$. In all experiments, air was introduced into the inner tube through a single orifice sparger $(d = 4\ mm)$. Figure 1 shows the schematic representation of this airlift reactor. Liquid phases were tap water and 0.5% aqueous solutions of methanol, ethanol, n-propanol, isopropanol and n-butanol. Table 2 presents the physical properties (surface tension, density, and viscosity) of these liquid systems. We employed Goetze's stalagmometer to determine the surface tension with an average error of $\pm$ 1.5%, densitometer APPAAR DMA46 to measurethe density with ±0.1 kg/m^3 accuracy, and Ostwald's viscometer to determine the viscosity with an average error of 1%. The

surface tension gradient with respect to concentration of the alcohol in the aqueous solutions ($d\sigma/dC_A$) was estimated from the slope of the experimental curve shown in Figure 2.

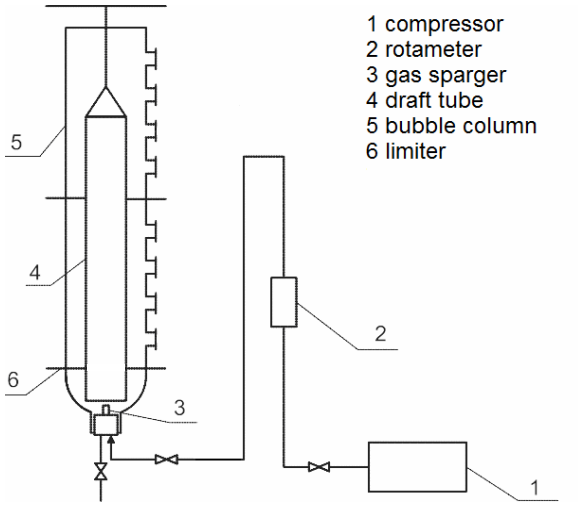

Figure 1. Schematic diagram of the experimental setup.

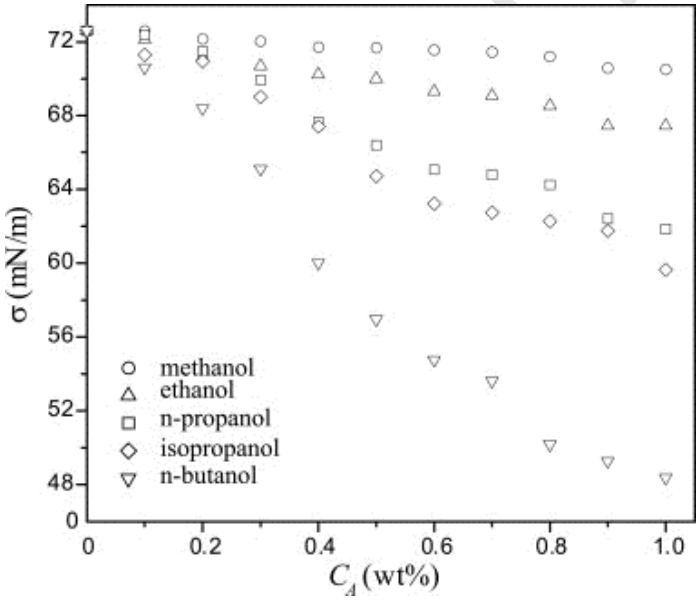

Figure 2. Surface tension in dilute alcohol solutions (Albijanic et al., 2007).

Table 2. Physical properties of the liquid phase at 20°C.

Liquid	σ (N/m)×10^3	$\lvert d\sigma/dC_A \rvert$ (Nm^2/mol)×10^3	ρ (kg/m^3)	μ (mPas)
tap water	72.76	-	998.2	1.003
0.5% methanol	71.52	0.008	996.9	0.996
0.5% ethanol	69.37	0.027	997.2	1.034
0.5% n-propanol	65.41	0.080	997.3	1.012
0.5% isopropanol	63.59	0.135	997.2	0.983

0.5% n-butanol	57.23	0.222		997.2	1.024

3.2. Liquid circulation time experiments

The experimental setup employed flow follower technique for recording the liquid circulation time, where a wax-coated glass bead facilitated the adjustment between the bead and liquid densities (Petrovic et al., 1991). Additionally, water glass covered the surface of the glass bead, changing the hydrophobicity of the bead from a hydrophobic to a fully hydrophilic surface state. The measured settling velocity of the glass bead in the static aqueous solutions in the downcomer was 2.5±2 cm/s. The velocity of the liquid represents the difference between the measured velocity and the settling velocity of the glass bead. The diameter of the glass bead was 4 mm, and the density of the glass bead (1034 kg/m^3) was determined by measuring its mass and calculating its volume. The bead travel/cycle time from-to a particular point was recorded as liquid circulation time. For each value of the superficial gas velocity, the experiment was repeated 30 times, maintaining a less than 7% error. In the following sections, an analysis of the data recorded during these experiments helps understand the contribution of physical properties of dilute alcohol solutions on the liquid circulation time.

3.3. Data analysis – a variable elimination approach

A formulation of the following hypotheses facilitates the assessment of the influence of an input variable (e.g. reagent A) on the output response (e.g. surface tension of water):

(1) H_0 the addition of reagent A affects the surface tension of pure water;

(2) H_1 the addition of reagent A does not affect the surface tension of pure water.

If the second hypothesis is valid, then statistically, there would only be a negligible difference between the surface tension of the aqueous solution of reagent A and the surface tension of pure water (i.e. the elimination of reagent A from water), and in that case, we can conclude that the addition of reagent A in water is not significant from an engineering standpoint. In other words, in this analysis, we eliminate one input variable, maintain the remaining input variables at their constant values, and repeat this procedure for all input variables to assess the influence of each input variable on an output response. Given this framework, the general form of a regression model in Equation (1) provides a starting point for this analysis:

$$y = f(x, \beta) \quad (1)$$

Here, $x = [x_1, x_2, \cdots, x_n]$ and $\beta = [\beta_1, \beta_2, \cdots, \beta_m]$ are the vectors representing input variables and regression coefficients, respectively; y is an output response; and f is a mapping function $x \rightarrow y$. To determine whether the corresponding regression coefficient β_i is significant, we formulate the following two hypotheses:

(1) $H_0(\beta_i = 0)$ the regression coefficient β_i is not significant,

(2) $H_1(\beta_i \neq 0)$ the regression coefficient β_i is significant.

An elimination of the corresponding coefficient β_i from the model determines the influence of coefficient β_i on the calculated output response y. In this context, we compare the following two cases:

Case I: All coefficients are included in the model (see Equation (1)).
Case II: One coefficient is zero $(\beta_i = 0)$, while others are kept constant (see Equation (1)).

It is important to note that the coefficient β_i would be significant, if the elimination of this coefficient (i.e. $\beta_i = 0$) from the model has a significant influence on the value of calculated y. Consequently, the hypothesis H_1 becomes valid, leading to a significant difference between the quality of curve fitting of Case I and Case II.

The quality of curve fitting can be assessed using the average relative deviation between the experimental and calculated values, i.e. average relative error (δ), parity plot diagram (the experimental values versus the calculated values), coefficient of determination (R^2), adjusted coefficient of determination (R_a^2), sum of square (SSE), and root mean squared error (RMSE). It is important to note that R^2 should not be used for the assessment of how well the experimental data fits the regression model because, in some cases, R^2 leads to misleading information subject to the limited range of input variables (Lazic, 2004). For example, Albijanic et al. (2007) examined whether the regression model could be used to describe the experimental data, and

found that when the average relative error was 3.1%, the coefficient of determination R^2 is calculated as 0.87 only.

The calculated average relative error (δ) for Case I is:

$$\delta = \frac{1}{n}\sum_{j=1}^{n}\left|\frac{y_e^j - y_c^j}{y_e^j}\right| \quad (2)$$

Here, n is the number of experimental data; y_e^j and y_c^j are the j^{th} experimental and calculated values, respectively. Given that this proposed method uses the non-linear regression, the average relative error is calculated using the k-fold cross-validation method to analyse the model overfitting. In k-fold cross-validation method, the available data is separated equally among *k* different groups, where $k-1$ groups of data are used for the training purpose, and one group is used for the testing purpose. This validation process is iterated over k number of times, generating k number of testing data based outcomes, which are then averaged to calculate an overall error for the model.

Similarly, the calculated average relative error $\delta(\beta_i = 0)$ for Case II is:

$$\delta(\beta_i = 0) = \frac{1}{n}\sum_{j=1}^{n}\left|\frac{y_e^j - (y_c^j)_{\beta_i}}{y_e^j}\right| \quad (3)$$

Here, $(y_c^j)_{\beta_i}$ represents the j^{th} calculated values for y, when the regression coefficient β_i is eliminated from the model, keeping other regression coefficients unchanged.

In order to assess the influence of the eliminated coefficient β_i (i.e. $\beta_i = 0$) on the calculated output response y, we can calculate the difference $B(\beta_i = 0)$ between δ and $\delta(\beta_i = 0)$, thus:

$$B(\beta_i = 0) = \delta(\beta_i = 0) - \delta \quad (4)$$

$b(\beta_i = 0)$ can be maintained within 0 and 1, as:

$$b(\beta_i = 0) = \frac{B(\beta_i=0)}{max[B(\beta_i=0)]} \quad (5)$$

Given that $max[B(\beta_i = 0)]$ is the largest among m available values (i.e. [$B(\beta_1$=0), $B(\beta_2$=0),…., $B(\beta_m$=0)]), the parameter $b(\beta_i = 0)$ is restricted to values between 0 and 1, and the higher the $b(\beta_i = 0)$ value, the more significant is the regression coefficient β_i. Similarly, the coefficient β_i is not significant if the following criterion is satisfied:

$$b(\beta_i = 0) < \varepsilon \quad (6)$$

Here, ε represents the threshold value that can be adopted to be less than the certain value (e.g. 0.05 or 0.1). This variable elimination approach guides in defining the contribution of liquid properties of dilute alcohol solutions on liquid circulation times.

4. Results and discussions

4.1. Liquid circulation time

Figure 3 presents the liquid circulation time as a function of superficial gas velocity. As shown in Figure 3, the circulation time curve can be divided into the three hydrodynamic regimes, marked as *Regime I*, *Regime II*, and *Regime III*. The changes in the slope of the line, representing these measurements, correspond to the transition from one regime to the next regime. This is in agreement with the visual observations of air bubbles in the downcomer. The presence of these hydrodynamic regimes has been recognized in other studies as well (Petrovic et al. 1991; Albijanic et al., 2007; Siljacki et al., 2010).

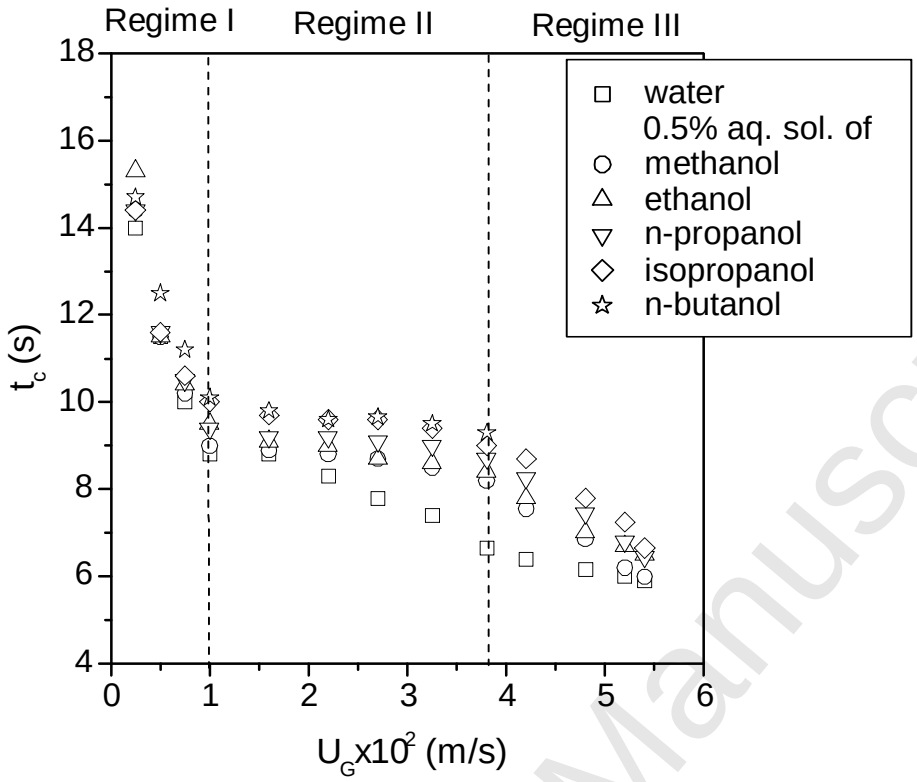

Figure 3. Liquid circulation time versus superficial gas velocity in the presence of tap water and different dilute alcohol solutions.

The zone of occurrence for *Regime I* corresponds to superficial gas velocity values less than 0.01 m/s ($U_G < 0.01\ m/s$), where liquid circulation was not sufficient to draw bubbles into the downcomer, and other studies (Jones et al., 1985; Petrovic et al., 1991; Albijanic et al., 2007) observed similar values for the superficial gas velocity in this regime. The zone of occurrence for *Regime II* corresponds to superficial gas velocity values greater than 0.01 m/s and less than 0.038 m/s ($0.01\ m/s < U_G < 0.038\ m/s$), where the liquid velocity is equal to the bubble rise velocity. In this regime, the entrainment of bubbles into the downcomer formed a stationary swarm of bubbles, which caused the additional hydrodynamic resistance for liquid circulation, leading to an almost constant liquid circulation time with the increase in the superficial gas velocity. Moreover, in this regime, a "loose" swarm of bubbles for water or a "dense" swarm of bubbles for the dilute alcohol solutions remained in the air-water dispersion. The entrainment of large bubbles ($3 - 5\ mm$) started at superficial gas velocity of $0.02\ m/s$ which agrees well with the results obtained in Weiland (1984). It should be noted that although bubble size distribution measurements were beyond the scope of this work, the bubble size was determined at superficial gas velocity of 0.02 m/s by taking into account the magnifying effect of the glass column. Finally, the zone of occurrence for *Regime III* corresponds to superficial gas velocity values

greater than 0.038 m/s ($U_G > 0.038\ m/s$), where liquid velocity is higher than the bubble rise velocity, and thus, the swarm of bubbles recirculates through the riser of the airlift reactor (Albijanic et al., 2007). The recirculation of bubbles started at the superficial gas velocity higher than $0.038\ m/s$, which is in agreement with the results obtained in Petrovic et al. (1991) and Albijanic et al. (2007).

Given these experimental observations, an analysis using paired sample t-test validates the existence of these hydrodynamic regimes. In this test, the null hypothesis assumes that the data in different regimes relates to the independent random samples from normal distributions with equal means and equal but unknown variance, and the alternative hypothesis establishes that the data in different regimes comes from populations with unequal means. Therefore, an acceptance of the alternative hypothesis (rejection of null hypothesis) validates the existence of the hydrodynamic regimes. Table 3 presents the results of this paired sample t-test. In Table 3, from the t-test values and the degree of freedom for all three comparisons, it is evident that the null hypothesis can be rejected with 95% confidence level. Consequently, the alternative hypothesis can be accepted, i.e. the data in all three regimes come from different statistical distribution, validating the creation of these regimes.

Table 3. Paired sample *t*-test among three different hydrodynamic regime data set.

	Paired samples *t*-test						
	Mean difference	Standard deviation	95% confidence of the difference		t-statistic value (*t*)	Significant level (2-tailed)	Degree of freedom
			Lower	Upper			
Regime I vs. Regime II	-0.0062	0.0106	-0.0120	-0.0003	-2.1206	0.0387	52
Regime II vs. Regime III	-0.0366	0.0113	-0.0431	-0.0300	-11.2182	5.1479E-15	48
Regime I vs. Regime III	-0.0428	0.0038	-0.0451	-0.0404	-37.1263	9.5894E-34	42

Figure 4 shows the relationship between the surface tension of dilute alcohol solutions and the liquid circulation time. As seen in Figure 4, the increase in surface tension reduces the liquid circulation time in the following order:

water < methanol < ethanol < n-propanol < isopropanol < n-butanol (7)

The effect of alcohols was insignificant at low superficial gas velocity (*Regime I*) because the amount of bubbles in the reactor was negligible. However, at higher superficial gas velocities (*Regime III*), a significant amount of bubbles was in the downcomer section of the airlift reactor and thus the effect of the coalescence inhibition of bubbles by alcohols was more pronounced, causing the differences between the investigated systems.

The coalescence inhibition of bubbles in dilute alcohol solutions occurs because adsorbed alcohol molecules on bubble surfaces orientate themselves with the hydrophilic part (i.e. hydroxyl group-OH^-) on the water side, and the hydrophobic part on the air side (i.e. hydrocarbon chain). In other words, the air-liquid interfaces of bubbles are charged which causes the repulsion among bubbles (Keitel and Onken, 1982). The coalescence inhibition of bubbles by alcohols is improved with the increase in the length of hydrocarbon chain of the aliphatic alcohols due to the formation of more stable rigid monolayer around bubbles (Keitel and Onken, 1982). The increase in the stability of the rigid monolayer reduces the bubble size and thus decreases bubble rise velocities (Keitel and Onken, 1982; Camarasa et al., 1999). Lesser bubble rise velocities improve the gas holdup in the downcomer section of draft tube airlift reactors which decreases the driving force for liquid circulation and consequently higher values for liquid circulation time (Albijanic et al., 2007; Siljacki et al., 2010).

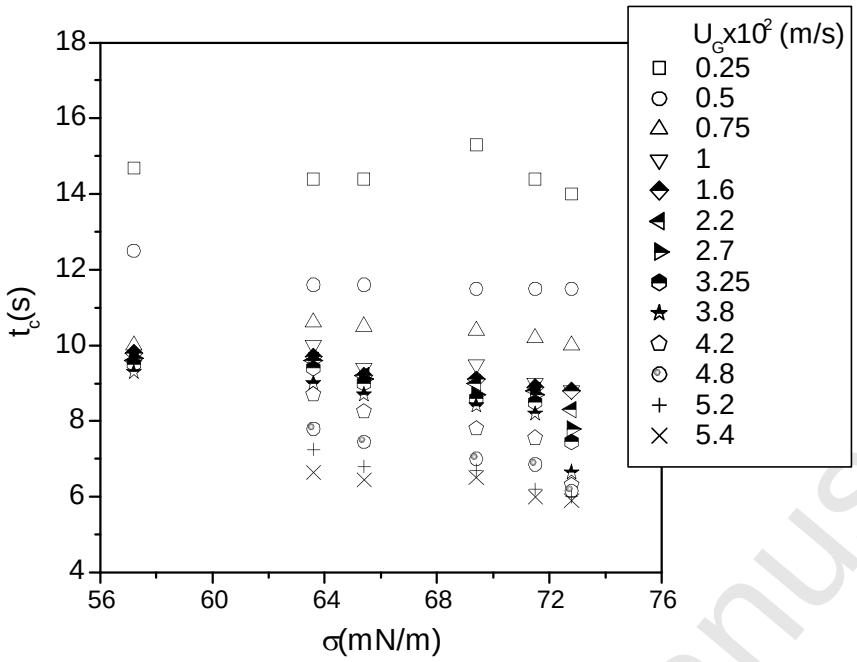

Figure 4. Liquid circulation time versus surface tension of tap water and dilute alcohol solutions.

Figure 5 compares the results in this and previous studies (Fields and Slater, 1983; Weiland, 1984; Petrovic et al., 1991; Kennard and Janekeh, 1991; Freitas and Teixeira, 1998; Albijanic et al., 2007). As seen in Figure 5, Weiland (1984) obtained relatively higher liquid circulation times probably because the sinter plate, used in his work, facilitates the formation of relatively more small bubbles in the downcomer, resulting in the increase in the liquid circulation time. By contrast, Kennard and Janekeh (1991) found relatively lower liquid circulation times probably because a shorter draft tube (0.5 m) in their work reduced the driving force for the liquid circulation.

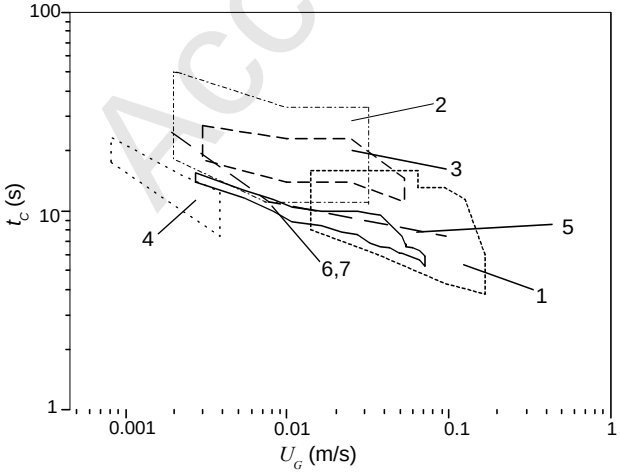

Figure 5. Liquid circulation time in draft tube airlift reactors. For the legend see Table 1 in which the reactor and the experimental details of previous studies are also provided.

4.2. Correlations

An application of LAB Fit software (Silva and Silva Cleide, 1999-2010) implementing the Levenberg–Marquardt algorithm (Bishop, 1997) facilitates the correlation analysis on the experimental data presented in Figure 3, and the proposed simple correlation predicts the liquid circulation time (t_c) measurements for all three regimes:

$$t_C = \beta_1 U_G^{\beta_2} \tag{8}$$

Table 4 illustrates the calculated regression coefficients, their standard errors, and *t*-values for each coefficient. Although Equation (8) can be used to describe the experimental data, this correlation does not account for the surface tension of dilute alcohol solutions (the only physical property of these solutions that is considerably different from pure water as seen in Table 2). Thus, two simple correlations that include either surface tension or surface tension gradient are as follows:

$$t_C = \beta_1 U_G^{\beta_2} \sigma^{\beta_3} \tag{9}$$

$$t_C = \beta_1 U_G^{\beta_2} \left(1 + \left|\frac{d\sigma}{dC_A}\right|\right)^{\beta_3} \tag{10}$$

Table 4 confirms that Equations (9) and (10) perform better in predicting the experimental data than Equation (8). It should be noted that apart from surface tension or surface tension gradient, the Bond number may also be worth using because this dimensionless number compares the surface tension with gravitational forces (Albijanic et al., 2006):

$$t_C = \beta_1 U_G^{\beta_2} Bo^{\beta_3} \tag{11}$$

where $Bo = \frac{D^2 \rho g}{\sigma}$ represents Bond number.

Table 4. Regression coefficients and model validation.

t_c (s)	Regime	β_1 (t value)	β_2 (t value)	β_3 (t value)	δ
Equation 8	I	2.334±0.174 (13.4)	-0.305±0.014 (22.1)		2.89
	II	8.326±0.563 (14.79)	-0.0126±0.013 (0.968)*		6.12
	III	0.626±0.357 (1.75)	-0.794±0.187 (4.23)		6.30
Equation 9	I	1.080±0.208 (5.18)	-0.304±0.014 (29.1)	-0.285±0.068 (4.19)	1.97
	II	1.304±0.412 (3.14)	-0.012±0.008 (1.41)*	-0.683±0.114 (5.92)	4.04
	III	0.016±0.008 (1.93)	-0.806±0.087 (9.28)	-1.353±0.166 (8.15)	2.84
Equation 10	I	2.163±0.130 (16.66)	-0.316±0.011 (-28.6)	0.177±0.083 (2.14)	2.13
	II	5.753±0.567 (10.13)	-0.103±0.027 (3.84)	0.774±0.110 (7.02)	3.60
	III	0.583±0.187 (3.11)	-0.795±0.106 (7.51)	0.140±0.213 (6.56)	3.17

*-Insignificant coefficients (95% confidence)

The 3-fold cross-validation method validates three correlations shown in Equations (8) - (10). In this method, the available data in each regime is divided equally into three groups, where two groups would be used for training and one group would be used for testing purposes. Tables 5, 6, and 7 present the error statistics in the 3-fold cross-validation method. The results in Tables 5, 6, and 7 demonstrate an overestimation of the values through proposed non-linear method. However, relatively lower values for mean squared errors, coupled with a slight difference between mean squared errors and error variances, applicable to these correlations over three regimes demonstrate that these correlations are capable enough to explain the data variability. Therefore, the developed correlations can be used for the prediction of the liquid circulation time. Although all three correlations can be used to describe the experimental data, Equation (10) is selected because the surface tension gradient includes the effect of alcohol concentration on the liquid circulation time. The experimental and predicted liquid circulation time using Equation (10) for all three hydrodynamic regimes are shown in Figure 6.

Table 5. Cross-validation error statistics of Equation (8).

	Regime I	*Regime II*	*Regime III*
Mean error	-0.00108	0.001801	-0.16703
Mean absolute error	0.423852	0.72569	0.506647
Mean squared error	0.288438	0.827735	0.440463
Error variance	0.300977	0.856274	0.434278
δ	3.85	8.51	7.53

Table 6. Cross-validation error statistics of Equation (9).

	Regime I	*Regime II*	*Regime III*
Mean error	-0.02805	-0.26863	-0.36569
Mean absolute error	0.255735	0.455323	0.371677
Mean squared error	0.125121	0.436633	0.216178
Error variance	0.12974	0.377041	0.086785
δ	2.25	5.37	5.45

Table 7. Cross-validation error statistics of Equation (10).

	Regime I	*Regime II*	*Regime III*
Mean error	-0.08729	-0.18618	-0.26688
Mean absolute error	0.303907	0.536014	0.508285
Mean squared error	0.150373	0.479540	0.374546
Error variance	0.148961	0.460219	0.319287
δ	2.63	6.10	7.41

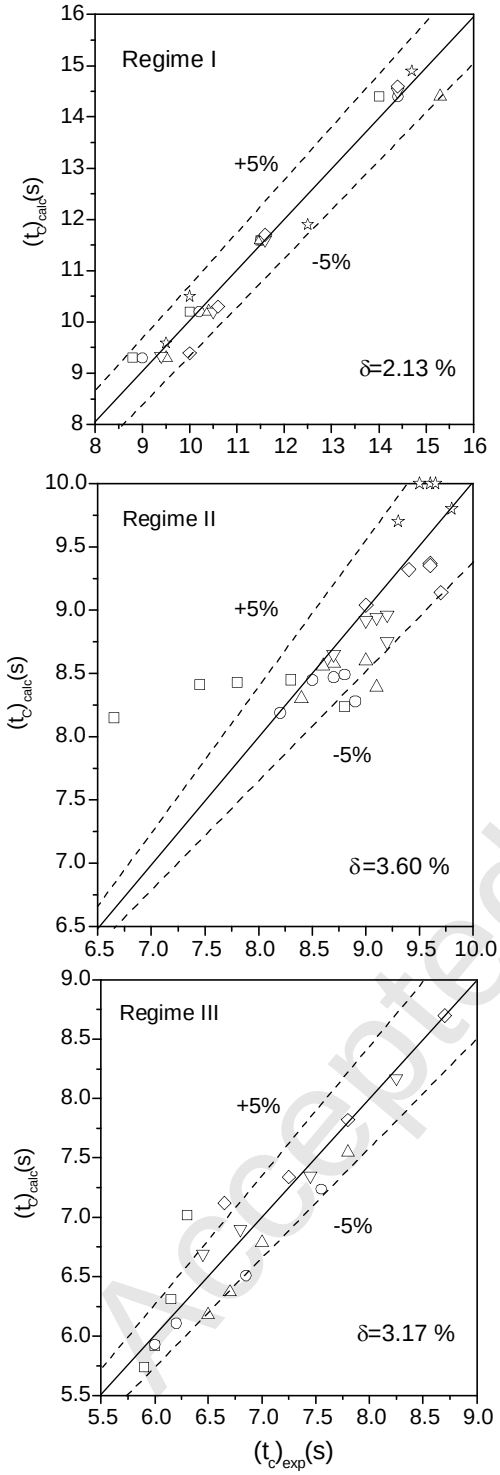

Figure 6. Calculated and experimental values of liquid circulation time.

4.3. Contribution of surface tension gradient on liquid circulation time

To evaluate the contribution of the surface tension gradient on liquid circulation time, we employ the method described in the methodology section of this paper. More specifically, the

contribution of the surface tension gradient of dilute alcohol solutions on the liquid circulation time, applicable for all hydrodynamic regimes can be determined using Equation (10).

In this context, for *Regime I*, the calculated regression coefficients are: $\beta_1 = 2.163$, $\beta_2 = -0.316$ and $\beta_3 = 0.177$. It is very important to highlight that β_2 and β_3 represent the effect of superficial gas velocity and surface tension gradient on the liquid circulation time, respectively.

The elimination method describes the effect of these three coefficients on liquid circulation time, as we will eliminate the influence of the coefficient by setting its value to zero. Thus, as an example, in *Regime I*, the following three cases are applicable:

(1) $\beta_1 = 0$, $\beta_2 = -0.316$, $\beta_3 = 0.177$, i.e. the coefficient β_1 is not significant if its elimination from the model $(\beta_1 = 0)$ does not affect the calculated liquid circulation time significantly.
(2) $\beta_1 = 2.136$, $\beta_2 = 0$, $\beta_3 = 0.177$, i.e. the coefficient β_2 is not significant if its elimination from the model $(\beta_2 = 0)$ does not affect the calculated liquid circulation time significantly.
(3) $\beta_1 = 2.136$, $\beta_2 = -0.316$, $\beta_3 = 0$, i.e. the coefficient β_3 is not significant if its elimination from the model$(\beta_3 = 0)$ does not affect the calculated liquid circulation time significantly.

Figure 7 shows the parity plot diagrams and calculated $\delta(\beta_i = 0)$ for all hydrodynamic regimes. It should be noted that $\delta(\beta_1 = 0)$ is zero regardless of the type of regime, and as such, it is not shown in Figure 7. As seen in Figure 7, for all three hydrodynamic regimes, $\delta(\beta_2 = 0)$ is higher than $\delta(\beta_3 = 0)$, indicating that the superficial gas velocity is more significant variable than the surface tension gradient of liquid phase. Indeed, for an application of the proposed method, it is not necessary to present the parity plot diagrams showing the deviation of all experimental points from their calculated values.

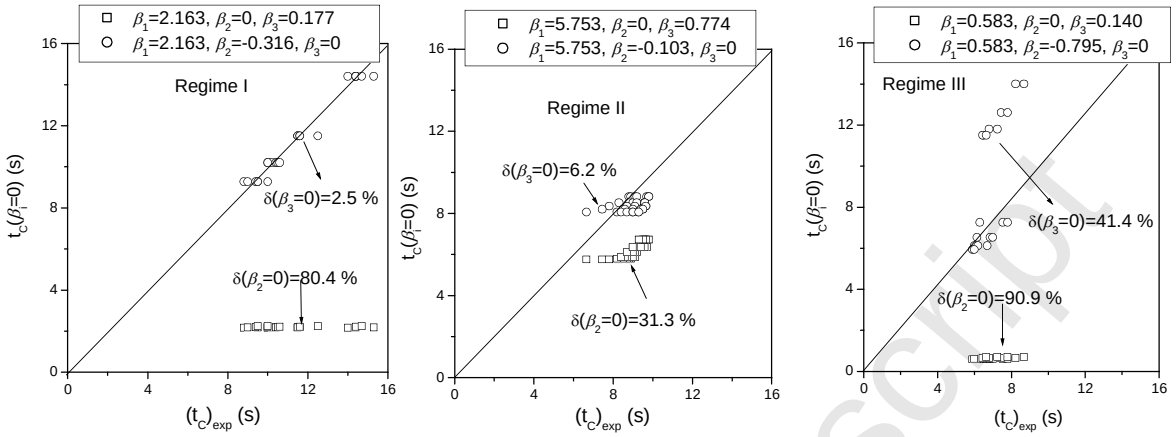

Figure 7. Comparison between experimental and calculated values for circulation time which is determined when β_2 or β_3 is eliminated from the model (i.e. β_i=0), while the values of other regression coefficients are kept constant.

Furthermore, Equations (4) and (5) calculate $b(\beta_i = 0)$, and Table 8 shows the relevant results of this parameter. Again, for all hydrodynamic regimes, the superficial gas velocity is more dominant variable than the surface tension gradient of liquid phase ($b(\beta_2 = 0) > b(\beta_3 = 0)$). This is particularly true in the case of *Regime I* because the amount of bubbles in the reactor is insignificant ($b(\beta_3 = 0) < 0.05$). Similarly, the influence of the surface tension gradient on the liquid circulation time could be neglected in *Regime II.* Table 8 also indicates that the impact of the surface tension gradient on the liquid circulation time decreases in the following order: *Regime III* > *Regime II* > *Regime I*. The reason is that the increase in superficial gas velocity causes a higher amount of bubbles in the downcomer section of the reactor and thus the effect of the surface tension gradient on the liquid circulation time is more noticeable.

Table 8. Calculated values of $b(\beta_i=0)$ using Equation (10)

Regime	$b(\beta_1 = 0)$	$b(\beta_2 = 0)$	$b(\beta_3 = 0)$
I	1.000	0.800	0.004*
II	1.000	0.287	0.030*
III	1.000	0.906	0.400

* Insignificant coefficient ($b(\beta_i=0) < 0.05$)

Additionally, it is worth analysing the rate of change in liquid circulation time as a function of both the superficial gas velocity and the surface tension gradient of liquid phase (i.e. two partial derivatives), as follows:

$$\left|\frac{\partial t_c}{\partial U_G}\right| = -\beta_1\beta_2 U_G^{\beta_2-1}\left(1+\left|\frac{d\sigma}{dC_A}\right|\right)^{\beta_3} \qquad (12)$$

$$\left|\frac{\partial t_c}{\partial(d\sigma/dC_A)}\right| = \beta_1\beta_3 U_G^{\beta_2}\left(1+\left|\frac{d\sigma}{dC_A}\right|\right)^{\beta_3-1} \tag{13}$$

$$\alpha = \frac{\left|\frac{\partial t_c}{\partial U_G}\right|}{\left|\frac{\partial t_c}{\partial(d\sigma/dC_A)}\right|} = \frac{-\beta_1\beta_2 U_G^{\beta_2-1}\left(1+\left|\frac{d\sigma}{dC_A}\right|\right)^{\beta_3}}{\beta_1\beta_3 U_G^{\beta_2}\left(1+\left|\frac{d\sigma}{dC_A}\right|\right)^{\beta_3-1}} = -\frac{\beta_2\left(1+\left|\frac{d\sigma}{dC_A}\right|\right)}{\beta_3 U_G} \tag{14}$$

Dividing Equation (12) by Equation (13) generates Equation (14) in which α is the measure of the strength of the effects due to the superficial gas velocity and the surface tension gradient. Figure 8 presents the average $(\bar{\alpha})$ values of α for each hydrodynamic regime. As seen in Figure 8, the superficial gas velocity is the dominant factor in all three hydrodynamic regimes $(\bar{\alpha} > 1)$ which is entirely in agreement with the conclusion obtained using the variable elimination approach explained in the methodology section of this paper. By contrast, Figure 8 also shows that the impact of the surface tension gradient decreases in the following order: Regime II > Regime III > Regime I. This conclusion partially agrees with the conclusion obtained using the variable elimination approach. The disagreement between these two approaches might be because the first approach quantifies the influence of one factor on the investigated variable while the second approach compares the influence of two factors on the investigated variable. It appears that both approaches should be applied to better understand the contribution of the surface tension gradient on liquid circulation time in draft tube airlift reactors.

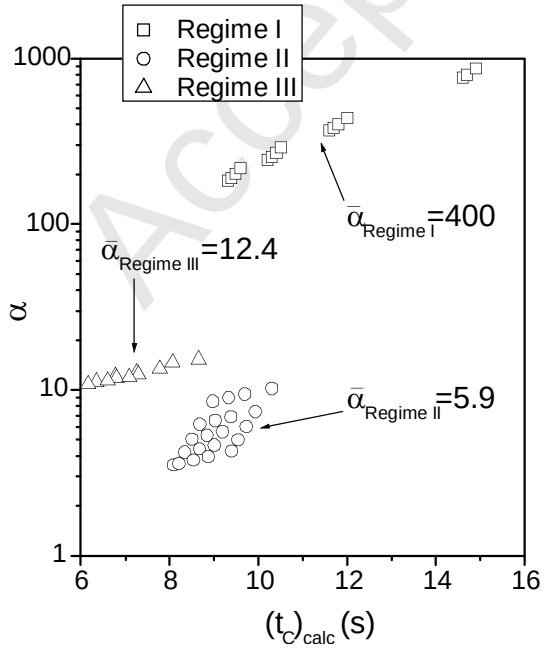

Figure 8. Influence of surface tension gradient on the liquid circulation time ($\overline{\alpha}$ represents the average value).

5. Conclusions

This paper evaluates the influence of surface tension gradient of alcohol solutions on liquid circulation time in a draft tube airlift reactor. Three different bubble regimes in the downcomer were observed: *Regime I* (no bubbles in the downcomer), *Regime II* (a stagnant swarm of bubbles in the downcomer) and *Regime III* (circulation of bubbles through the reactor). An analysis using a paired sample t-test confirms the existence of these regimes. The coefficient elimination approach quantifies the contribution of surface tension gradient of dilute alcohol solutions and superficial gas velocity on the liquid circulation time. The second approach determines the rate of change in the liquid circulation time as a function of both the superficial gas velocity and the surface tension gradient. The results show that the superficial gas velocity was more significant variable than the surface tension gradient for all three hydrodynamic regimes. Nevertheless, the influence of the surface tension gradient on the liquid circulation time should be taken into account particularly in *Regime II*. Further work is required to evaluate the contribution of added alcohols on other hydrodynamic variables and mass transfer coefficients for different sections of this airlift reactor.

References

Albijanic, B., Havran, V., Petrovic, D., Djuric, M., Tekic, M., 2007 Hydrodynamics and Mass Transfer in a Draft Tube Airlift Reactor with Dilute Alcohol Solutions. AIChE Journal. 53, 2897– 2904.

Albijanic, B., Djuric, M., Petrovic, D. and Tekic, M., 2006. Prediction of gas hold-up for alcohol solutions in a draft-tube bubble column, Acta Periodica Technologica, 37, 71– 81.

Albijanic, B., 2006. Investigation of alcohol addition on hydrodynamics and mass transfer in a draft tube airlift reactor. Master thesis, University of Novi Sad, Novi Sad, Serbia.

Al-Masry, W.A., Dukkan, A.R., 1997. The role of gas disengagement and surface active agents on hydrodynamics and mass transfer characteristics of airlift reactors. Chem. Eng. J. 65, 263–271.

Bishop, C.M., 1997. Neural Networks for Pattern Recognition. Oxford University Press, New York, pp 504.

Camarasa, E., Vial, C., Poncin, S., Wild, G., Midoux, N., Bouillard, J., 1999. Influence of coalescence behaviour of the liquid and of gas sparging on hydrodynamics and bubble characteristics in a bubble column. Chem. Eng. Process 38, 329–344.

Chakravarty, M., Singh, H.D., Baruah, J.N., Iyengar, M.S., 1974. Liquid velocity in a gas-lift column. Indian. Chem. Eng. 16, 17–22.

Chisti, M.Y., 1989. Airlift Bioreactor, Elsevier Applied Science, London, New York, pp 256.

Freitas, C., Teixeira, J.A., 1998. Effect of liquid-phase surface tension on hydrodynamics of a three-phase airlift reactor with an enlarged degassing zone. Bioprocess Eng. 19, 451–457.

Jones, A.G., 1985. Liquid circulation in a draft-tube bubble column, Chem. Eng. Sci. 40, 449–462.

Keitel, G., Onken, U., 1982. Inhibition of bubble coalescence by solutes in air/water dispersions, Chem. Eng. Sci. 37 (11), 1635–1638.

Kennard, M., Janekeh, M., 1991. Two- and three-phase mixing in a concentric draft tube gas-lift fermentor. Biotechnol. Bioeng. 38, 1261–1270.

Krishna, R., Urseanu, M.I., Dreher, A.J., 2000. Gas hold-up in bubble columns: influence of alcohol addition versus operation at elevated pressures. Chem. Eng. Process. 39, 371–378.

Morgan, E., 1991. Chemometrics: experimental design. John Wiley and Sons, New York.

Petrovic, D., Posarac, D., Dudukovic, A., Skala, D., 1991. Hydrodynamics and mass transfer in a draft tube bubble column. J. Serbian Chem. Soc. 56, 227–240.

Sijacki, I., Colovic, R., Petrovic, D. Lj., Tekic, M. N., Duric, M., 2010. Diluted Alcohol Solutions in Bubble Columns and Draft Tube Airlift Reactors with a Single Orifice Sparger: Experiments and Simple Correlations. J. Chem. Technol. Biotechnol. 85, 39–49.

Silva, W.P., Silva Cleide M.D.P.S. LAB fit curve fitting software V 7.2.47 (1999–2010), available at www.labfit.net.

Weiland, P.,1984. Influence of draft tube diameter on operation of airlift loop reactors. German Chem. Eng. 7, 374–385.